Journal of Magnetism and Magnetic Materials 323 (2011) 620–630

Contents lists available at ScienceDirect

Journal of Magnetism and Magnetic Materials

journal homepage: www.elsevier.com/locate/jmmm

Strain induced phase separation on $La_{0.5}Ca_{0.5}MnO_3$ thin films

A. Antonakos [a,*], E. Liarokapis [a], G.H. Aydogdu [b], H.-U. Habermeier [b]

[a] Department of Physics, National Technical University, GR-15780 Athens, Greece
[b] Max-Planck-Institute for Solid State Research, Stuttgart D-70569, Germany

ARTICLE INFO

Article history:
Received 21 February 2010
Received in revised form
7 September 2010
Available online 27 October 2010

Keywords:
Manganites thin films
Colossal magnetoresistance
Raman spectroscopy
Phase separation

ABSTRACT

The effect of epitaxial strain on $La_{0.5}Ca_{0.5}MnO_3$ films of various thicknesses grown on $SrTiO_3$, $SrLaAlO_4$, and $SrLaGaO_4$ substrates is studied by Raman spectroscopy, magnetic, and resistivity measurements. The transport and magnetic properties as well as Raman spectra of the films are affected by epitaxial strains. The energy of the $A_g(2)$ mode and the tilting angle of the MnO_6 octahedra is affected by the strain imposed by the substrate. In the spectra of the films deposited on the (1 0 0) $SrTiO_3$ substrate strong Jahn–Teller (JT) modes appear, which couple with charge-ordering. In all other films these modes are suppressed and no additional Raman lines are present at low temperatures contrary to the bulk compound. The low frequency continuum scattering decreases at low temperatures indicating a coupling with both the charge and orbital transitions. Comparison of the Raman spectra with the magneto-transport properties suggests an interpretation in terms of a strain induced phase separation between ferromagnetic metallic and antiferromagnetic insulating states.

© 2010 Elsevier B.V. All rights reserved.

1. Introduction

During the past decades the empirical discovery of colossal magnetoresistance (CMR) [1,2] effect in doped rare earth manganites $R_{1-x}A_x$ MnO_3 (R: a trivalent rare-earth ion; A: a divalent alkaline-earth ion) [7] has attracted much attention. The underpinning physics has found to be related with strong electron correlation and the coupling of the electron system to the lattice via the Jahn–Teller (JT) effect. The doping level leads to the mixed valance of the manganese ion (coexistence of Mn^{+3}/Mn^{+4} ions in a suitable ratio). The complex phase diagram of the manganites with doping can be described by a JT induced charge-localization competing with the magnetic interactions (double exchange—DE model [8]), charge, orbital and spin ordering [9]. The control of the transport and magnetic properties by internal (doping concentration, average atomic radius $\langle r_A \rangle$) and external perturbations (temperature, pressure, and magnetic field) is crucial for the application of manganites to devices [3–6]. In thin films grown on a substrate, the epitaxial strain caused by the lattice–substrate mismatch [10,11] is an additional control parameter affecting physical properties of thin films [12]. The lattice distortion [13–16] and the strain relaxation mechanism induce phase separation and inhomogeneities the films [17,18].

$La_{1-x}Ca_xMnO_3$ (LCMO) has a very rich phase diagram of ground states with competing order parameters [19]. The parent compound is $LaMnO_3$, which belongs to the family of rotationally distorted perovskites [20] and is an antiferromagnetic (AF) insulator. The bulk compound at the phase boundary with $x=0.5$ is a paramagnetic (PM) insulator and at low temperatures undergoes first a ferromagnetic (FM) and simultaneously AF and charge ordering (CO) transitions (T_C=225–265 K and T_N=130–160 K), respectively [21]. The formation of the charge- and orbital-ordered (COO) AF insulating states were firstly observed in LCMO ($x=0.5$) [22,23]. There are several studies that investigated the phase separated LCMO compound at several doping levels [24–34]. The phase separation phenomenon is regarded as an important factor for the large resistivity change accompanied by the first order IM transition [35].

Raman scattering is a very sensitive tool for studying lattice distortions, electronic excitations, phase transitions, etc. These effects have an influence on the phonon characteristics and the low frequency electronic continuum scattering [36–38]. An extensive amount of Raman data exist for the LCMO series and an assignment for most of the phonons has been proposed [20,39]. In addition, there are detailed studies of the bulk $La_{0.5}Ca_{0.5}MnO_3$ compound [21,41,40] but to the best of our knowledge little work has been done on thin films [42].

In the present work, we study the strain effects on the transport and magnetic properties and the phase separation of the LCMO system. It is demonstrated that different substrates can be exploited as a tool to obtain thin films with adjustable electronic and magnetic properties while for this chemical composition the bulk compound is at the boundary between a FM metal and a CO/AF insulator. We show that small perturbations due to strain can cause changes in structural properties and manipulate the phase separation and the coexisting phases in the thin films.

* Corresponding author. Tel.: +30 2107722950; fax: +30 2107723312.
E-mail address: tantonak@central.ntua.gr (A. Antonakos).

0304-8853/$ - see front matter © 2010 Elsevier B.V. All rights reserved.
doi:10.1016/j.jmmm.2010.10.030

2. Experimental

The $La_{0.5}Ca_{0.5}MnO_3$ (LCMO) films were deposited on (0 0 1) oriented $SrLaGaO_4$ (SLGO), $SrLaAlO_4$ (SLAO), (1 1 1) and (1 0 0) oriented $SrTiO_3$ (STO) single crystal substrates by pulsed laser deposition (PLD) at 1073 K and with an oxygen pressure of 0.4 mbar. After deposition, films were annealed at 1173 K for 30 min at ambient oxygen pressure. The PLD system has an excimer laser with KrF gas mixture operating at the wavelength of 248 nm. The laser fluence and pulse frequency were fixed to 1.6 J/cm^2 and 5 Hz, respectively. The thicknesses of the films (290 and 145 nm) were adjusted by calculating the ablation period during the growth process, determined by calibration of the depositions. The error in film thickness was around 10%. Before deposition, single crystal substrates were cleaned in ultrasonic baths of acetone and ethanol, then, they were mounted to the sapphire sample holder.

Determination of the epitaxial relationship between film and substrate and the phase analysis were carried out by X-ray diffraction (XRD) using the Cu Kα radiation ($\lambda = 1.54056$ Å). Pole figures were measured in a Philips X'Pert MRD diffractometer equipped with an Eulerian cradle. The $2\theta-\omega$ scans at various inclination angles (ψ) were performed with a four-circle Bruker D8 Discover diffractometer. The temperature dependence of magnetization was investigated by a Quantum Design MPMS superconducting quantum interference device (SQUID) magnetometer during field cooling (FC) and zero-field cooling (ZFC). During ZFC, samples first were cooled to 5 K then field was applied to sample. Afterwards, magnetization was measured in the heating process up to 300 K. During FC, samples were cooled from 300 down to 5 K in the same field. The magnetic field (100 G) was oriented parallel to the film surface. Resistivities of the films were measured with evaporated chromium gold contacts using four-point probe method within a temperature range between 5 and 300 K at 10^{-7} A.

The polarized Raman spectra were obtained using a T64000 Jobin Yvon triple spectrometer, equipped with a liquid nitrogen cooled charge coupled device (CCD) and a microscope. The 514.5 nm line of an Ar^+ laser was used for excitation at low power, which was kept fixed during the measurements at the level of ~ 0.2 mW on the surface of the film. The spectral resolution was less than 1 cm^{-1} as checked by the 871.74 nm line of a fluoride lamp. Raman spectra of the film were measured at a temperature region from 20 to 295 K. A backscattering geometry was used, with the sample placed under the microscope with $\times 100$ magnification.

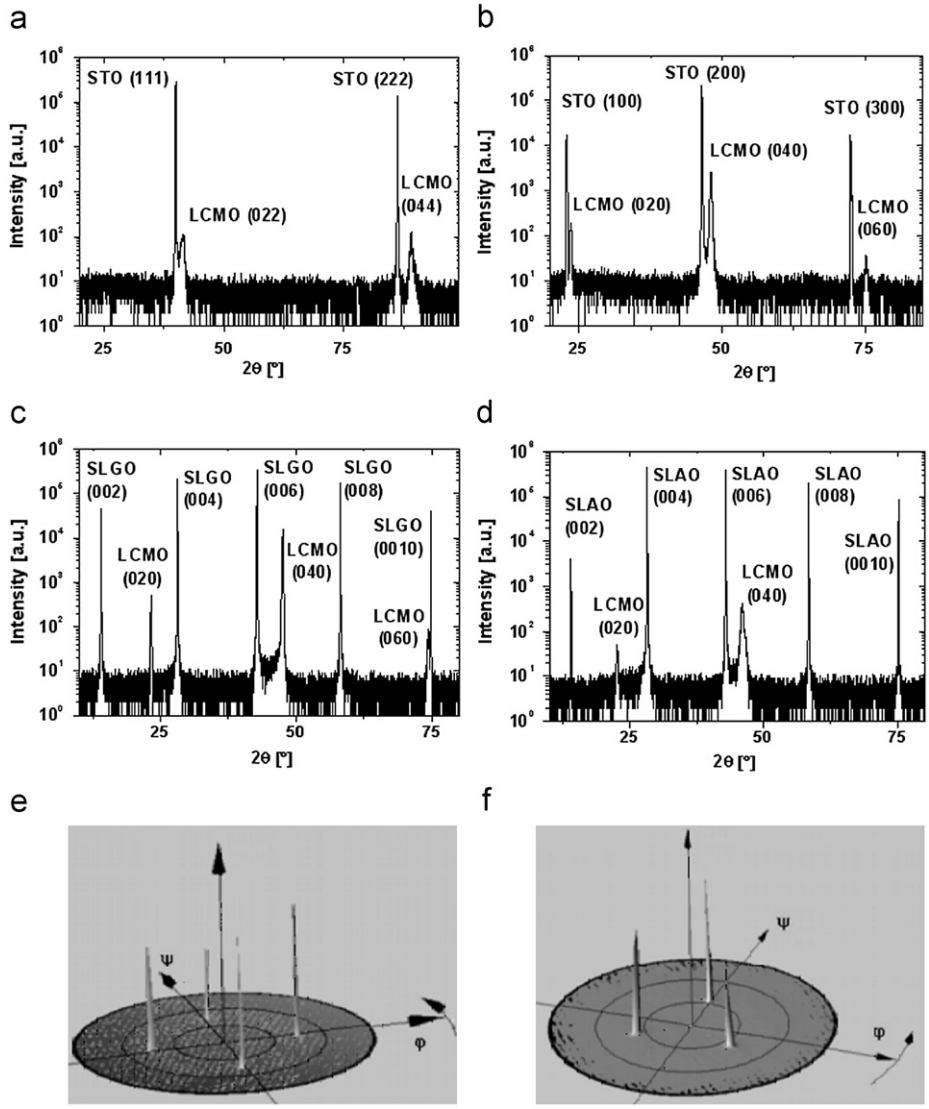

Fig. 1. Representative $2\theta-\omega$ scans for the 290 nm films on (a) (1 1 1) STO, (b) (1 0 0) STO, (c) (0 0 1) SLGO, (d) (0 0 1) SLAO; representative pole figures for films on (e) (1 0 0) STO, (0 0 1) SLGO and SLAO (f) (1 1 1) STO substrates.

Download English Version:

https://daneshyari.com/en/article/1801064

Download Persian Version:

https://daneshyari.com/article/1801064

Daneshyari.com